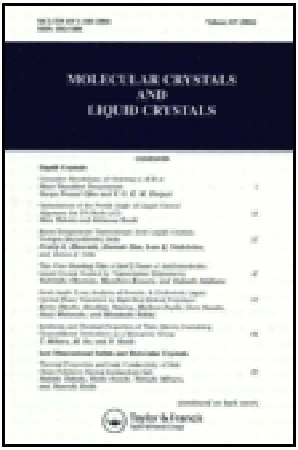

Molecular Crystals and Liquid Crystals

Publication details, including instructions for authors and subscription information:
http://www.tandfonline.com/loi/gmcl20

Cano-Grandjean Wedge at Weak Surface Anchoring

V. A. Belyakov [a]

[a] L.D. Landau Institute for Theoretical Physics, Moscow, Russia

Version of record first published: 22 Sep 2010

Mol. Cryst. Liq. Cryst., Vol. 480, pp. 262–277, 2008

ISSN: 1542-1406 print/1563-5287 online
DOI: 10.1080/15421400701826704

Cano-Grandjean Wedge at Weak Surface Anchoring

V. A. Belyakov
L.D. Landau Institute for Theoretical Physics, Moscow, Russia

Theoretical study of the chiral liquid crystal (CLC) director distribution in a wedge shape cell with weak surface anchoring is presented. It is found that for a sufficiently short pitch CLC the well known defect lines separating the wedge area differing by the number of director half turns N at the wedge thickness may be replaced by nonsingular walls. It should be noted that the term "weak surface anchoring" really is related to the large values of the dimensionless parameter $S_d = K_{22}/Wd$*, where* K_{22} *is the elastic twist modulus, d is the layer thickness and W is the depth of the surface anchoring potential. So, at any strength of the anchoring a sufficiently thin layer (small d) insures the conditions of "weak surface anchoring". At sufficiently thick area of the wedge the well known picture of the defect lines separating the wedge areas differing by the number of director half turns restores. The calculations of the director distribution in a wedge shape cell with infinitely strong anchoring at one surface and finite anchoring strength at the second one performed for the two sets of model anchoring potentials reveal qualitative difference in the director distributions for the Rapini-Papoular-like and B-like model surface anchoring potentials. The results show that the experimentally distinguishable details of the director distribution in the wedge area with nonsingular walls allow one to obtain information on the shape of the surface anchoring potential and estimate the energy of the defect lines replacing the nonsingular walls.*

Keywords: Cano-Grandjean wedge; nonsingular walls; weak surface anchoring

INTRODUCTION

The behaviour of the structure of confined chiral liquid crystal (CLC) with a finite surface anchoring strength under action of continuously changing external agent (temperature, electric or magnetic field etc.) attracts now considerable attention due to the interesting physics of the phenomenon [1,2] and its direct connection to liquid crystal

Address correspondence to V. A. Belyakov, L.D. Landau Institute for Theoretical Physics, Kosygin str. 2, 117334 Moscow, Russia. E-mail: bel@landau.ac.ru

applications [3]. A typical feature of the corresponding behaviour is not only smooth changes of the structure in some range of the external agent values but also jump like changes for the definite values of the continuously changing agent and a hysteresis of these jump-like changes points if the agent variation is changed in the opposite direction. For example, the jump of the pitch in the cell initiated by a smooth variation of the temperature [1,4,5], electric or magnetic field [6,7,8] or mechanical rotation of the surface limiting a cell [9] may occur. As it was shown [2,10] for a relatively weak surface anchoring the corresponding jump points and the hysteresis are directly dependent on the shape of the anchoring potential and its strength, so experimental studies of the related phenomena may be useful for the reconstruction of the actual surface anchoring potential. Quite recently another phenomena connected to the shape of the anchoring potential were studied. These are the temporal dynamics of the pitch jump [2,10] and the motion of a non-singular wall dividing the areas of different values of the pitch in a planar CLC layer [11,12,13]. These studies revealed also the dependence of the temporal evolution of the jump on the shape and the strength of anchoring for a relatively weak surface anchoring. More over, the distribution of director in the non-singular wall (moving or motionless) is also dependent on the shape of surface anchoring potential [12].

All mentioned phenomena are connected with the large angular deviation of the director at the layer surface from the alignment direction. It is why they are suitable for determination of the potential shape. Recall that at the small angular director deviation angles from the alignment direction any surface anchoring potential has to be quadratic on the deviation angle, so the phenomena connected with small director deviation angles from the alignment direction are insensitive to the shape of the surface anchoring potential. As a first step in the direction of restoring of the actual shape of the anchoring potential new model surface anchoring potentials [2,10] were introduced.

It should be noted here that the term "relatively weak surface anchoring" really is related to the large values of the dimensionless parameter $S_d = \mathbf{K}_{22}/W\mathbf{d}$, where K_{22} is the elastic twist modulus, d is the layer thickness and W is the depth of the surface anchoring potential. So, at any strength of the anchoring a sufficiently thin layer (small d) insures the conditions of "relatively weak surface anchoring".

We shall study below the phenomenon of the same nature, as mentioned above, occurring when a varying external agent is the thickness of the planar CLC layer. The simplest experimental way to study what is happening with the director distribution in the layer at continuous variation of the layer thickness is investigation of the phenomenon in a wedge cell. So, what follows further is devoted to description of the director distribution in the wedge cell for a finite strength of surface anchoring at the wedge surfaces.

PLANE LAYER

Before proceed to a wedge shape sample examine variation of the director structure for a planar cholesteric layer with a finite strength of the surface anchoring under the changing of its thickness and fixed all other parameters of the problem. Specifically, we shall examine the behaviour of the cholesteric helix in a planar layer with a finite anchoring strength at one of its surfaces and infinite anchoring at the other. Assume that the alignment directions are coinciding at the both surfaces (see Fig. 1 considering the deviation angle φ at one of the surfaces to be identically equal to zero) and, as in the previous works [1,4,5,6], assume that the pitch jump mechanism is connected with the director overcoming the anchoring barrier at the surface. The problem is very similar to the corresponding problems related to the temperature [1,4,5,14] and the field [6–8] induced variation of the director structure for a planar cholesteric layer with a finite strength of the surface anchoring, so we shall remind here only the main equations describing the problem (the details may be found in [1,4,5,6–8]).

The free energy of a homogeneous layer may be presented in the following form

$$F(T) = W_s(\varphi) + (K_{22}/2d)[\varphi - \varphi_0(d)]^2, \tag{1}$$

where φ is the angle of the director deviation from the alignment direction at the surfaces with finite anchoring, $\mathbf{W_s(\varphi)}$ is the surface anchoring potential, $\mathbf{K_{22}}$ is the elastic twist modulus, d is the layer thickness, the angle $\boldsymbol{\varphi_0(d)}$ gives the angle of the director deviation from the

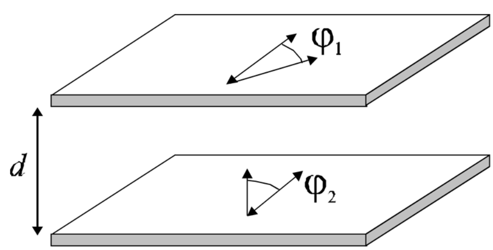

FIGURE 1 The case of nonidentical anchoring at the surfaces of a cholesteric layer.

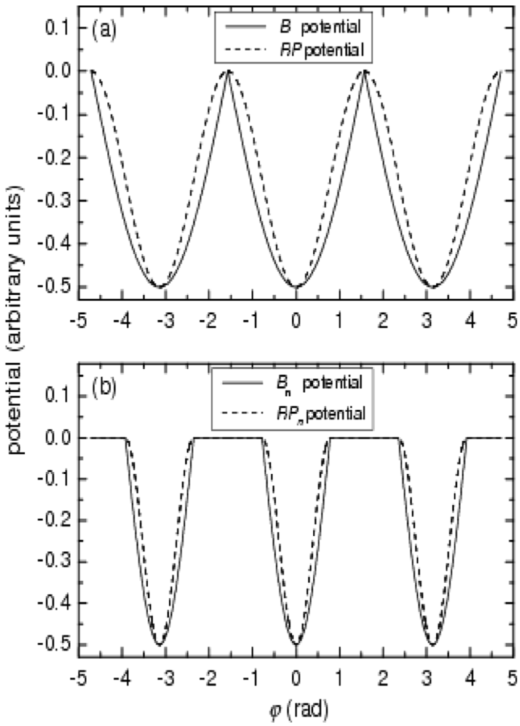

FIGURE 2 Qualitative plots of the Rapini-Papoular and the B and the Rapini-Papoular like (R-P_n) and the B like (B_n)-potentials.

alignment direction at the surface with finite anchoring if the anchoring at this surface were absent at all, i.e. the director free rotation angle, which is determined only by the layer thickness variations ($\boldsymbol{\varphi_0}(\mathbf{d}) = 2\pi d/p$, where p, or natural pitch, is the value of pitch in a bulk cholesteric).

One obtains the equation determining the angle φ at the surface of the layer as a function of d by minimization of Eq. (1). The corresponding eqution is

$$\ldots\ldots\ldots \partial W_s(\varphi)/\partial_\varphi + (K_{22}/d)(\varphi - \varphi_0) = 0 \tag{2}$$

Solving this equation for the different model anchoring potentials $\mathbf{W_s(\boldsymbol{\varphi})}$ (see Appendix) one finds that the angle φ being a function of the thickness d is also dependent on the dimensionless parameter $\mathbf{S_d} = K_{22}/Wd$, where W is the depth of anchoring potential, and the specific of its functional dependence on d and $\mathbf{S_d}$ is different for the different model anchoring potentials [2,10]. Note that the parameter $\mathbf{S_d}$ is fixed for the problem with unchanged layer thickness and is variable in our problem, so it is naturally to introduce a new parameter which does not change at the layer thickness variations. It is convenient to introduce a new dimensionless parameter $l_p = L_p/p$, where $L_p = K_{22}/W$ is, so called, the penetration length [15]. Introducing this parameter one gets the following form of the Eq.(2):

$$\partial W_s(\varphi)/\partial\varphi + W(S_d\varphi - 2\pi\, l_p) = 0 \tag{3}$$

Like in the case of the fixed layer thickness the solution of Eqs.(2,3) is a smooth function of the thickness d (or parameter S_d) in some ranges of the thickness d with abrupt jumps of φ at definite thicknesses of the layer for which φ reaches the critical value φ_c.

We shell investigate below except Rapini-Papoular (R-P) also recently introduced in [2,11], so called, B-potential (A.1) and comment briefly on the narrow angular width R-P-like (A.4) and B-like (A.2) model surface anchoring potentials introduced in [10].

The Eq. (3) for the B-potential reduces to the following form:

$$\sin\varphi + 2\ S_d\varphi - 4\pi l_p = 0, \tag{4}$$

with the critical angle φ_c to be equal $\pi/2$.

The analysis of the problem (for the temperature and field variations see [5–7]) shows that in a layer with homogeneous distribution of the director over the layer surface a smooth changing with the layer thickness d of the director deviation angle from the alignment direction φ is possible while φ is less than the critical angle φ_c. Upon achieving by φ of the critical value φ_c a jump-like change of the pitch occurs and a transition to a new configuration of the helix differing by one in the number of the director half-turns at the layer thickness N occurs. The critical value φ_c corresponds to achieving by the configuration with N director half-turns in the layer of an instability point and reducing to zero of the potential barrier between director configurations with N and N + 1 half-turns.

The results of numerical solution of the Eqs. (4) for the B-potential are presented at Figures 3, 4. In the calculations the value of the parameter l_p was assumed to be close to its value determined experimentally in [14] (the parameter S in [14] is equal identically to $4\pi l_p$). The Figure 3 presents the variations of the director half-turns number N in the layer versus the layer thickness (in the number of the natural pitches at the layer thickness) for increasing and decreasing the layer thickness. It, along with smooth changes of N, reveals jumps of N at some points. The two curves are not coinciding. It happens that at

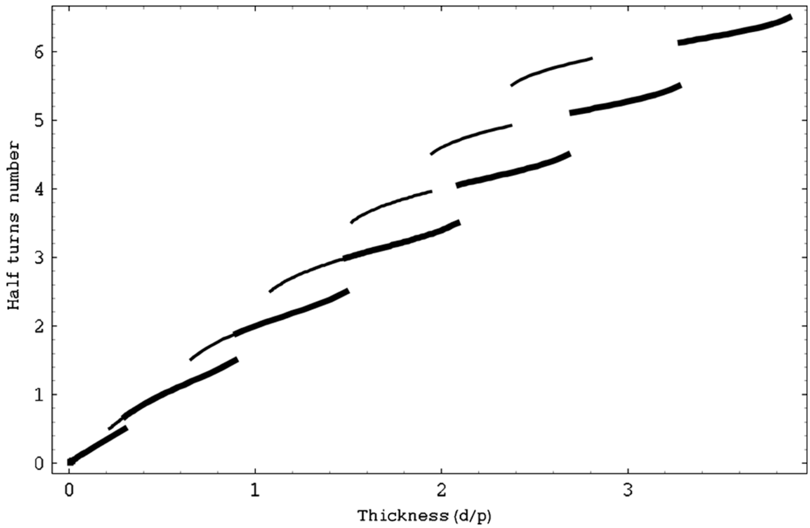

FIGURE 3 Change of the half-turns number in a plane layer versus the layer thickness (d/p) for B-potential (bold line at increasing, narrow line at decreasing of the thickness, $l_p = 0.5$).

increase of the layer thickness the helical spiral in the layer is undertwisted and at decrease of the layer thickness it is overtwisted compared to the free helical spiral and the jump points are not coinciding for the opposite directions of the layer thickness variation. The Figure 4 presents an example of a possible hysteresis loop at inversion of the direction of the layer thickness variation. If an inversion of the thickness d change begins at the point corresponding to the topper bold liner at the Figure 3 a jump of the pitch at decreasing of d does not coincide with the jump point of the bold lines (see Fig. 4 where the directions of d variations are marked by arrows) but corresponds to the jump point for the narrow lines. If little after the jump at decreasing of d one inverses the direction of d change again the increase of the half-turns number will follow the second from the top bold line at the Figure 4. By this way one can get a simplest hysteresis loop related to the $\Delta N = 1$. If the points of d change inversion corresponds to the $\Delta N > 1$ the shape of hysteresis loop becomes more complicated and may include many jumps depicted at the Figure 3.

If the described jump happens in a limited area of the layer surface the director distribution over the layer surface become inhomogeneous and the wall (interface between the configurations with N and $N + 1$ half-turns of the director) occurs. Typically [12] the wall thickness

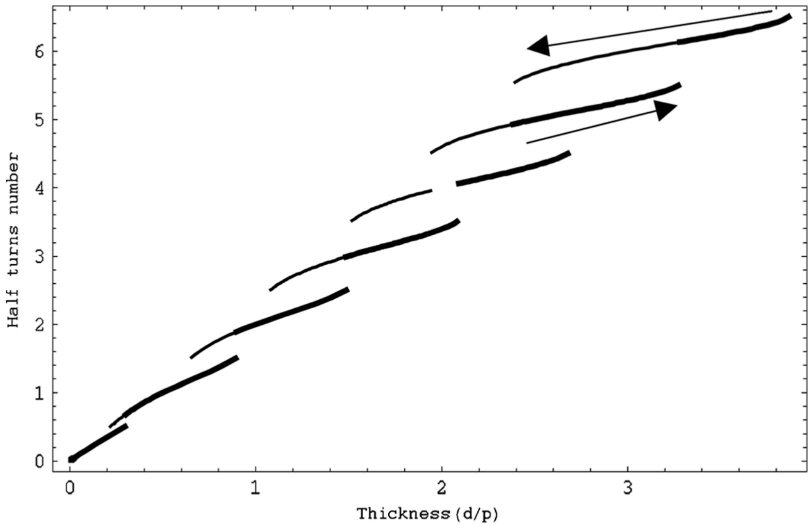

FIGURE 4 Hystersis in the variation of the half-turns number in plane layer versus the layer thickness (d/p) for B-potential (bold line at increasing, narrow line at decreasing of the thickness, $l_p = 0.5$) shown around d/p = 3 (The directions of the thickness variations are also shown by the arrows).

along the layer surface is much less than the layer thickness. The wall begins its motion in the direction of the N configuration, because the free energy of the N configuration per a unit layer area is higher than the corresponding value for the N + 1 configuration [11,12]. However this wall may be motionless, the case of main interest below. It happens if the free energy of the N configuration per a unit layer area is the same as the free energy for the N + 1 configuration. In our case these situations of the motionless walls take place at the thicknesses of the layer which result in the director orientations at the surface at free its rotation (without the anchoring) being perpendicular to the alignment direction, i.e. $d/p = (2n + 1)/4$, where $n = 0,1,2\ldots.$ and p is the pitch in a bulk sample. At these points the director at the layer surface with a finite anchoring makes the angles φ_e and $-\varphi_e$ relative to the alignment direction for the N and N + 1 configuration, respectively. Naturally, these angles φ_e are dependent on the layer thickness at which a motionless wall may exist. The jump of the director orientation at the layer surface is equal to $\pi - 2\varphi_e$ i.e. it is dependent on the layer thickness at which the motionless wall exists. One derives from (4) the following equation for φ_e:

$$\sin\varphi_e + 2\ S_{de}\varphi_e - 4\pi\ l_p = 0, \tag{5}$$

where S_{de} is the value of S_d corresponding to the layer thickness at which a motionless wall may exist. In our consideration, in which all parameters of the problem except the thickness d are fixed a motionless wall exists for discreet thicknesses of the layer. One has to search for the solution of Eq. (5) for the discreet values of S_d, i.e. for S_{de}, and it is why the values of φ_e found from (5) are also discreet. However, if the fixed in our case parameters vary the value of φ_e become a continuous function of the varying parameter. Just a such case of the varying parameter (natural pitch p) was examined in [12]. So we may use the calculations performed in [12] to find the needed for us discreet solutions of Eq. (5).

So, related to a motionless wall thevalues of equilibrium angle φ_e(measured from the alignment direction at the surface with the finite anchoring) and the angular jump at the wall $\Delta\varphi = \pi - 2\varphi_e$ may be found as from Figures 3, 4 so from Figures 5,6 (Figs. 4, 8 in [12]) if one takes into account that the corresponding thicknesses of the layer d_e at Figures 3, 4 are determined by the following expression

$$d_e/p = (2n + 1)/4, \quad (6)$$

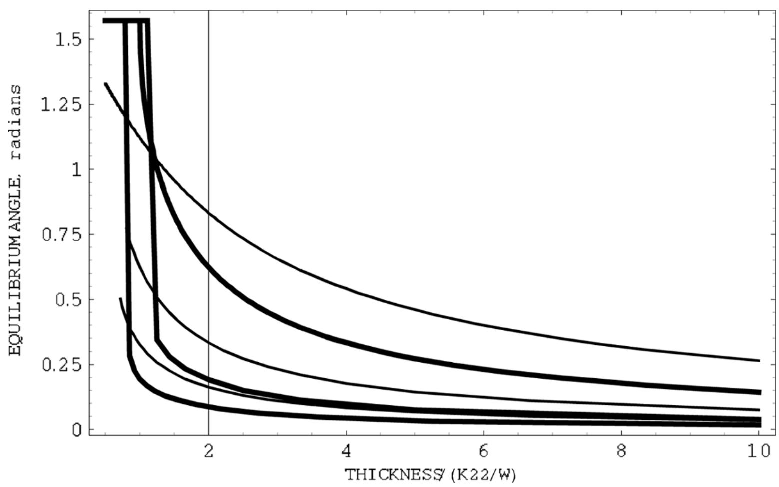

FIGURE 5 Equilibrium director deviation angle φ_e calculated versus the sample thickness normalized by the penetration length K_{22}/W for R-P-like (bold lines) and B-like potentials (for the narrow potentials $n = 2,3$; the smaller n the higher is the corresponding curve) [12]. The curves related to the present study are the top bold (R-P-potential) and the top narrow (B-potential).

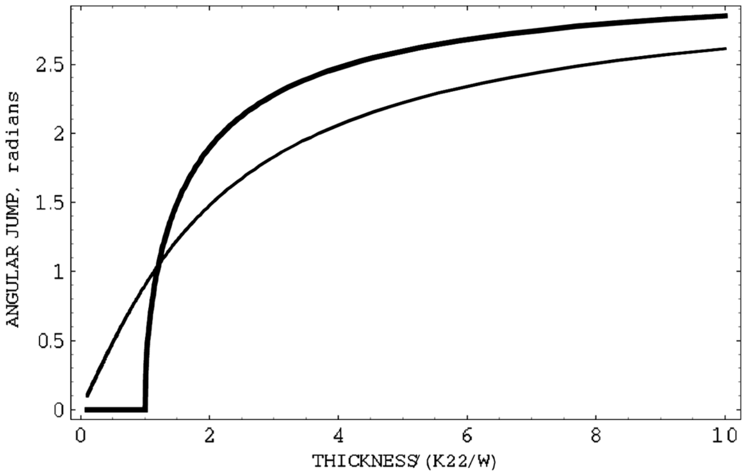

FIGURE 6 Angular jump of the director at wall versus the layer thickness d normalized by the penetration length K_{22}/W for R-P-(bold line) and B-surface anchoring potentials [12].

where $n = 0,1,2\ldots$ and p is the natural pitch of CLC (the pitch in a bulk sample). At Figure 5 φ_e is plotted versus $1/S_d$, i.e. versus $(d/p)/l_p$. So, the values of φ_e and $\Delta\varphi$ corresponding to the solutions of Eq. (5) are presented in the Figures 5, 6 at the values of the abscissa $1/S_{de} = (2n+1)/(4l_p)$. For the presented here calculations of the director twisting in the layer versus the thickness with $l_p = 0.5$ (Figs. 3, 4) the corresponding values of the abscissa at Figures 5, 6 determining φ_e and $\Delta\varphi$ are $n + 1/2$.

It should be mentioned that the calculations presented here don't take into account the thermal fluctuations of the director orientation. As was shown in [1] the thermal fluctuations are essential for thick layers. The fluctuations result in decreasing of the jump hysteresis with the layer thickness increase and in complete disappearance of the hysteresis for sufficiently thick layers.

WEDGE

In principle, the pitch variations in a plane layer versus the layer thickness studied in the previous section may be directly measured in the experiment. However, it looks that a wedge-shape sample gives a more easy way to do this. So, we shall now study how the behaviour of the director configuration at variations of the planar layer thickness reveals itself in the Cano-Granjean wedge. We shall assume below that the wedge angle is small enough and the formulas obtained above for a planar layer of variable thickness may be applied locally to the wedge. It also will be assumed as above that the alignment direction is the same for the both surfaces (with infinite and finite anchoring) limiting the wedge.

As one sees at Figures 3, 4 the jumps of the pitch in the layer at variation of its thickness d happen at the layer thicknesses for which the free energies of the N and $N+1$ director configuration are not equal because the jump positions don't coincide with the values given by (6). In a wedge the director configurations just at the both sides of a Cano-Granjean line have to correspond to an equilibrium state of the system (we don't consider transitional phenomena and assume that one examines the wedge at the time when a liquid crystal in the wedge has reached already a steady state with a minimal free energy). For a such steady state the free energies of the N and $N+1$ director configuration at the both side of the wall have to be locally equal. It means that in the wedge the walls exist at the wedge thicknesses determined by Eq. (6) so the parameters S_{de} and φ_0 in the Eqs. (2–3) are known. Therefore we have to calculate smooth director reorientations at the surface between the two consecutive walls in the range determined by the consecutive values of d_e given by (6) for n and $n+1$. For a plane layer a homogeneous bistable state occurs at the edges of these ranges being associated with a possible jump of the director orientation between the two N and $N+1$ layer configurations of equal free energies. In a wedge the jump is substituted by a wall which for sufficiently thin part of the wedge may be non-singular [12].

The calculation results of the dependence of the pitch on the local wedge thickness (d/p) in a wedge with finite anchoring at one surface and infinite anchoring at the second one are presented at Figures 7, 8 for R-P (see A.4 at $n=1$) and B (A.1) anchoring model potentials, respectively. The parameter l_p was assumed to be close to its value determined experimentally in [14]. One sees a qualitative difference in the corresponding dependences for R-P and B potentials at the thin part of the wedge. If for the B-potential the walls (pitch jumps) occur for the all local thicknesses determined by Eq. (6) for the R-P-potential the walls (pitch jumps) at the thin part of the wedge may be absent and appear at the thickness d above some critical value. This means that the first jump may occur at $n > 0$ in the Eq. (6) or even at n more than the several first integer numbers. What is concerned of the wall (jump) positions for the R-P-potential they are coinciding with the corresponding wall (jump) positions for the B-potential (which differ by one half of the pitch p in the local thickness, i.e. are determined by the Eq. (6) at $n > 0$). As was already mentioned in a wedge the jumps

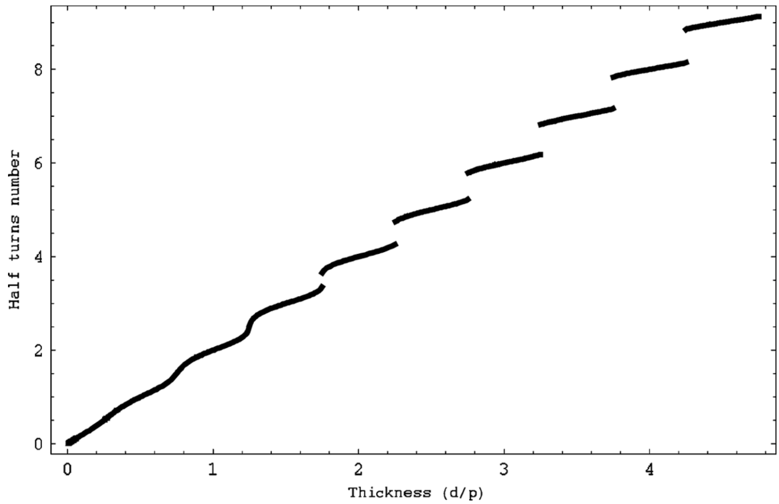

FIGURE 7 Variation of the half-turns number in the wedge versus the local wedge thickness (d/p) for R-P-potential ($l_p = 1.5$).

(see Figs. 7, 8) are substituted by the walls. It actually means that in the wedge at the positions of the jumps depicted at the Figures 7, 8 fast, however continuous, variations of the director orientation occur.

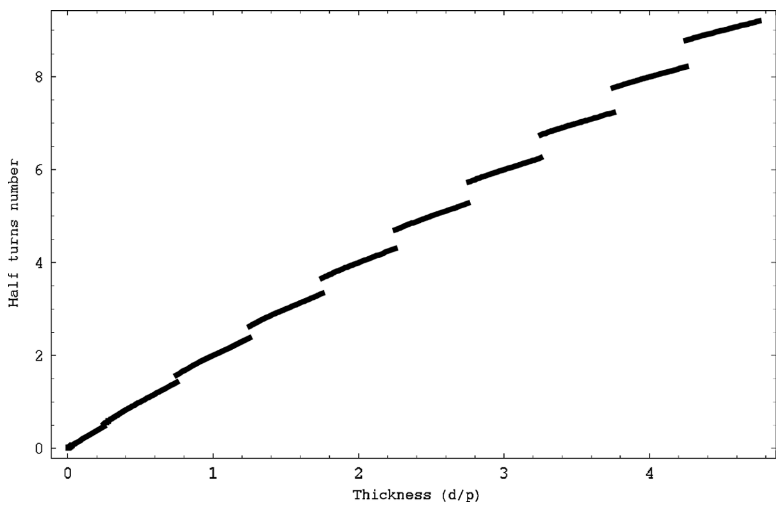

FIGURE 8 Variation of the half-turns number in the wedge versus the local wedge thickness (d/p) for B-potential ($l_p = 1.5$).

The walls for R-P and B potentials reveal also differences in the shape of director distribution in the wall and in the wall width [12]. Nevertheless the wall width is typically less than the local wedge thickness [12].

ON WALLS CORRESPONDING TO $\Delta N = 2$

It should be noted that a well known structure of the Cano-Granjean lines at a strong surface anchoring [14] corresponds to the jumps of pitch with $\Delta N = 1$ at the first lines (thin part of the wedge) and at the subsequent lines (thick part of the wedge) corresponds to the jumps with $\Delta N = 2$. The same transition from $\Delta N = 1$ to $\Delta N = 2$ structure of the wall at the thick part of the wedge one has to expect in the present approach to the Cano-Granjean wedge structure. The base for these expectations is connected with the fact that for a sufficiently thick layer (small S_d) a jump with $\Delta N = 1$ does not correspond to a transition of the configuration to the state with minimal free energy [5]. So at achieving of some thickness of the layer the transition of the configuration to the state with a minimal free energy corresponds to $\Delta N = 2$.

The same tendency is supported by the consideration of the energy gain connected with the substitution of the walls with $\Delta N = 1$ by the walls with $\Delta N = 2$ for a thick part of the wedge. At this substitution the number of walls with $\Delta N = 2$ has to be twice less than the number of walls with $\Delta N = 1$ at the same length of the wedge. So, one has to compare the energy of two walls with $\Delta N = 1$ with the energy of a wall with $\Delta N = 2$. The energy of the wall is given by the formula $E_w = 3\mathbf{K_w}V/2$ [12], where $\mathbf{K_w}$ is the elastic modulus related to the problem and approximately equal to $\mathbf{K_{22}}/2$ and V is the dissipation integral which may be estimated [12] by the formula $V = (d/3)\int(d\varphi/dx)^2]dx$, where the coordinate x directed along the surface and is perpendicular to the wall. The calculation of this integral [12] results in $V = (1–2\varphi_e/\pi)^2(2d/3L)$ for $\Delta N = 1$and in $V = (1 + 2\varphi_e/\pi)^2(2d/3L)$ for $\Delta N = 2$, where L is the wall thickness and the quantities $2\varphi_e/\pi$, being little different for $\Delta N = 1$ and $\Delta N = 2$, are small relative to 1 for a sufficiently large thickness d. One can easily see that for sufficiently large d the energy of two walls with $\Delta N = 1$, i.e. $2(1–2\varphi_e/\pi)^2(2d/3L)$, becomes larger than the energy of a wall with $\Delta N = 2$, i.e. $(1 + 2\varphi_e/\pi)^2(2d/3L)$. The presented arguments show that at some thickness the walls with $\Delta N = 1$ have to be substituted by the walls with $\Delta N = 2$. However for obtaining of the precise thickness d of this substitution one has to perform more accurate calculations.

One has also another question related to the problem under consideration. It is: what kind of the wall, non-singular or singular, is corresponding to the director configuration change with $\Delta N = 2$? The answer to this question is connected with the comparison of the energies of the non-singular and singular Cano-Granjean lines [12] and demands also more accurate calculations what is out of the scope of the present investigation.

CONCLUSION

The performed study shows that the non-singular Cano-Grandjean lines can be experimentally observed for the low value of the anchoring strength achieved already in the experiment. For example, a low depth of the anchoring potential $W = 10^{-5}\,J/m^2$ was reported in [14,16]. The corresponding value of the parameter l_p in [14] is 1.5 therefore the first Cano-Grandjean lines in the wedge have to be non-singular if the parameters of the problem are the same as in [14]. There are indications that a much lower surface anchoring energy may be reached and a large number of non-singular Cano-Grandjean lines can be experimentally observed. Namely, the value of W lower than $3 \times 10^{-10}\,J/\,m^2$ was reported in [17] however in the cited paper a degeneration of the alignment direction was observed. It seems quite probable that the degeneration of the alignment direction may be removed by the price of a moderate increase of the W value reported in [17] (see [18]).

It is interesting to present rough estimates of the local wedge thicknesses at which a non-singular Cano-Grandjean line is substituted by a singular Cano-Granjean line and a wall with $\Delta N = 1$ is substituted by a wall with $\Delta N = 2$. The local thickness of the wedge where a wall with $\Delta N = 1$ is substituted by a wall with $\Delta N = 2$ may be estimated as a wedge thickness for which due to the anchoring the director rotation angle in the wedge is less than the free rotation angle by 2π or the number of free half-turns at the local wedge thickness exceeds the number of half-turns at the same thickness in the wedge by 2 (see Figs. 7, 8). One easily finds (see [5]) that it happens if $S_d \leq 1/8\pi$, i.e. $d/p \geq 8\pi l_p$. The corresponding estimate for the local wedge thicknesses at which a non-singular Cano-Granjean line is substituted by a singular Cano-Grandjean line (see [12] and the previous section) is $d/p > (5\pi)^2 l_p$. The comparison of this two estimates give rise to the hopes that a non-singular wall with $\Delta N = 2$ may be also observed if a sufficiently low anchoring strength will be reached.

It should be noted that the study of the Cano-Grandjean lines in a wedge with a weak surface anchoring open a simple way to get some information useful for the physics of liquid crystals. First of all the information may be used for restoring the shape of anchoring potential (see the Figs. 7, 8 revealing different structure of the Cano-Grandjean lines for different anchoring potentials). Another possibility which looks as a very attractive is the experimental determination of the energy of a defect line based on determination of the distance in the wedge (local thickness) for which the energy of non-singular wall becomes equal to the defect line energy and the substitution of a non-singular wall by a singular line takes place. The open question is the dynamics of the Cano-Grandjean lines. For this problem, however, the results related to a planar layer of varying thickness may be useful. Namely, the positions of jumps in the layer (see Figs. 3, 4) determine stability limits for the positions of the non-singular walls in the wedge, i.e. maximal possible deviation of the wall from the equilibrium positions determined by the Eq. (6). And finally, study of a wedge with the surface anchoring corresponding to a narrow anchoring potential [2] promises a possibility of qualitatively different structures of the Cano-Grandjean lines at thin part of the wedge in comparison with their structure for the potentials with the angular width of the well equal to π. For example, walls corresponding $\Delta N = 1/2$ may be possible for the narrow potentials. What is concerned of the experimental investigation of the considered Cano-Grandjean lines the most common kind of such investigations, the optical one giving integrated information over the thickness, may be supplemented by a new local method which ensures now the space resolution at the scale of $1\,\mu m$ [16,19].

The work is supported by the RFBR grant 06-02-16287.

APPENDIX

NEW MODEL SURFACE ANCHORING POTENTIALS

For the purpose of easy reference we give below expressions for the Rapini-Papoular (R-P), so called, B-potential recently introduced in [2], and the narrow angular width R-P-like and B-like model surface anchoring potentials introduced in [10,11] (see Fig. 2).

The B-potential [2] is given by the formula:

$$W_s(\varphi) = -W[\cos^2(\varphi/2) - 1/2], \quad \text{if } -\pi/2 < \varphi < \pi/2. \tag{A.1}$$

The period of the B-potential is π, i.e. $\mathbf{W_s}(\boldsymbol{\varphi} + \pi) = \mathbf{W_s}(\boldsymbol{\varphi})$.

The narrow B_n-potential (n > 1):

$$W_s(\varphi) = -W(\cos^2(n\varphi/2) - 1/2), \quad \text{if } -\pi/2n < \varphi < \pi/2n. \qquad (A.2)$$
$$W_s(\varphi) = 0, \quad \text{if } \pi/2n < |\varphi|\, \pi/2,$$

and continued periodically to $|\varphi| > \pi/2$ (see Fig. 2), according to the relation $W_s(\varphi) = W_s(\varphi - \pi)$, where $n > 1 (n = 1$ corresponds to the B-potential).

The free energy (1) for the B_n-potential accepts the following form:

$$F(T)/W = -(\cos^2(n\varphi/2) - 1/2) + (S_d/2)[\varphi - \varphi_0(T)]^2$$
$$\text{if } -\pi/2n < \varphi < \pi/2n, \qquad (A.3)$$
$$F(T)/W = (S_d/2)[\varphi - \varphi_0(T)]^2 \quad \text{if } \pi/2n < |\varphi| < \pi - \pi/2n.$$

By a similar way, as B_n-potential, is determined the narrow R-P_n-potential:

$$W_s(\varphi) = -(W/2)\cos^2(n\varphi), \quad \text{if } -\pi/2n < \varphi < \pi/2n, \qquad (A.4)$$
$$W_s(\varphi) = 0, \quad \text{if } \quad \pi/2n < |\varphi| < \pi/2,$$

and continued periodically to $|\varphi| > \pi/2$ (see Fig. 2), according to the relation $W_s(\varphi) = W_s(\varphi - \pi)$, where $n > 1$ ($n = 1$ corresponds to the R-P-potential).

The free energy (1) for the R-P_n-potential accepts the following form:

$$F(T)/W = [-\cos^2(n\varphi) + S_d[\varphi - \varphi_0]^2]/2, \quad \text{if } -\pi/2n < \varphi < \pi/2n,$$
$$F(T)/W = (S_d/2)[\varphi - \varphi_0(T)]^2, \quad \text{if } \quad \pi/2n < |\varphi| < \pi - \pi/2n. \qquad (A.5)$$

One has to keep in the mind that the B-potential, being an alternative to the R-P-potential, is some simple and convenient idealization of the physically acceptable surface anchoring potential. Namely, the B-potential has a discontinuous first derivative at the maximum point (edge of the potential well,) and thus the curvature is infinitely large. However, one should accept it as a simple model for a class of possible potentials with a very sharp maximum (i.e. very large but finite curvature at the well edge). What is concerned of the R-P-like and B-like surface anchoring potentials with a narrow angular potential well they are natural generalizations of the R-P- and B-potentials which may be useful in the case of a liquid crystal limited, for example, by a single crystal. In this case more than one alignment direction exists, so the widths of anchoring potential well corresponding to each alignment direction have to be less than π. If one alignment direction is much "stronger" than all other ones, it is possible in the first approximation to neglect by all surface anchoring wells except the one related to the "strong alignment direction". As a result one obtains the potential of R-P_n -and B_n-type discussed here.

REFERENCES

[1] Belyakov, V. A., Oswald, P., & Kats, E. I. (2003). *JETP*, *96*, 915.
[2] Belyakov, V. A., Stewart, I. W., & Osipov, M. A. (2004). *JETP*, *90*, 73.
[3] Kim, J., Yoneya, M., & Yokoyama, H. (2002). *Nature*, *420*(6912), 159.
[4] Zink, H. & Belyakov, V. A. (1996). *MCLC*, 265, 445; (1995). *JETP Letters*, *63*, 43.
[5] Belyakov, V. A. & Kats, E. I. (2000). *JETP*, *91*, 488.
[6] Belyakov, V. A. & Kats, E. I. (2001). *JETP*, *93*, 380.
[7] Belyakov, V. A. (2002). *JETP Letters*, *76*, 88.
[8] Belyakov, V. A. & Semenov, S. V. *Proceedings of SPIE, Vol. 6023* (SPIE, Bellingham, WA, 2005) 6023–08.
[9] Belyakov, V. A. & Kuczynski, W. (2005). *MCLC*, *265*, 445.
[10] Belyakov, V. A., Stewart, I. W., & Osipov, M. A. (2005). *Phys.Rev. E*, *71*, 051708.
[11] Belyakov, V. A., Oswald, P., & Kats, E. I. (to be published).
[12] Belyakov, V. A., Osipov, M. A., & Stewart, I. W. (2006). *J.Phys.: Condens. Matter*, *18*, 4443.
[13] Belyakov, V. A. & Kuczynski, W. *MCLC* (to be published).
[14] Zink, H. & Belyakov, V. A. (1997). *JETP*, *85*, 488.
[15] a) de Gennes, P. G. & Prost, J. (1993). *The Physics of Liquid Crystals*, Clarendon Press: Oxford.
b) Oswald, P. & Pieranski, P. (2000). *Les cristaux liquides: concepts et propriétés physiques illustrées par des expériences*, Gordon and Breach Science Publishers: Paris.
[16] Smalyukh, I. I. & Lavrentovich, O. D. (2002). *Phys. Rev. E*, *66*, 051703.
[17] Ramdane, O. Ou., Auroy, Ph., Forget, S. et al. (2000). *Phys. Rev. Lett.*, *84*, 3871.
[18] Il'in, A., Ouskovs, E., Reznikov, Yu., Blanc, C., Nobili, M., Antonova, K., Buluy, O. et al. (2006). *Journal of the SID, 14*/7, 603.
[19] Smalyukh, I. I. & Lavrentovich, O. D. (2003). *Phys. Rev. Lett.*, *90*, 085503.